

New Allyldithiocarbimates: Synthesis, Structure and Antifungal Activity against *Phakopsora pachyrhizi* and *Hemileia vastatrix*

Antonio E. C. Vidigal,^a Mayura M. M. Rubinger,^b *^a Lucas F. da Silva,^b
Laércio Zambolim,^b Arthur B. D. Pereira,^a Silvana Guilardi,^c Rafael A. C. Souza^c
and Javier Ellena^d

^aDepartamento de Química, Universidade Federal de Viçosa, 36570-977 Viçosa-MG, Brazil

^bDepartamento de Fitopatologia, Universidade Federal de Viçosa, 36570-977 Viçosa-MG, Brazil

^cInstituto de Química, Universidade Federal de Uberlândia, 38400-902 Uberlândia-MG, Brazil

^dInstituto de Física de São Carlos, Universidade de São Paulo, 13566-590 São Carlos-SP, Brazil

Twelve tetraphenylphosphonium allyldithiocarbimates were synthesized and fully characterized by high-resolution electrospray ionization mass spectrometry (HR-ESI-MS), infrared and nuclear magnetic resonance (NMR) spectroscopies. The spectroscopic data indicated that the allyldithiocarbimate anions present Z configuration, as confirmed by X-ray crystallography. These new compounds inhibited the germination of *Phakopsora pachyrhizi* and *Hemileia vastatrix* at very low doses, with IC₅₀ (concentration to achieve 50% of inhibition of spore germination) values ranging from 0.028 to 0.166 mmol L⁻¹, and IC₉₀ (concentration to achieve 90% of inhibition of spore germination) values varying from 0.156 to 0.528 mmol L⁻¹. Allyldithiocarbimate salts are lead compounds for the development of new antifungals for coffee leaf rust and Asian soybean rust, devastating plant diseases with limited control options.

Keywords: allyldithiocarbimate, crystal structure, antifungal activity, *Hemileia vastatrix*, *Phakopsora pachyrhizi*

Introduction

Dithiocarbamates (Figure 1) are protectant fungicides extensively used in agriculture. For example, Ziram, whose active principle is the zinc dimethyldithiocarbamate (ZDMC), is used either single or in mixtures with more specific systemic fungicides.¹ Even though the metal-dithiocarbamates do not present high toxicity when compared to other fungicides, the literature² reports that Ziram and other zinc-dithiocarbamates increase the

intracellular levels of Zn²⁺, which might induce apoptosis and other adverse events. In addition, it has been recently discovered that Ziram inhibits androgen production and steroidogenic enzyme activities in rat Leydig cells, *in vitro*.³

Although similar to the dithiocarbamates, the dithiocarbimates (Figure 1) are much less studied and have no commercial applications yet. In previous research, it was found that *N*-R-sulfonyldithiocarbimate metal complexes (metals: Zn, Ni, Sn) inhibit the mycelial growth of *Colletotrichum*, *Botrytis* and *Alternaria* spp., *in vitro*.⁴⁻⁷ The potassium salts of the free dithiocarbimate ligands are not stable enough in solution for accurate biological studies.⁴ Attempting to synthesize stable metal-free organic dithiocarbimates derivatives, we have recently prepared the first examples of allyldithiocarbimates, via nucleophilic substitution reactions of aromatic sulfonyldithiocarbimates with Morita-Baylis-Hillman (MBH) adducts derivatives. These compounds were also active, inhibiting the mycelial growth of *B. cinerea*, *in vitro*.⁸

Considering the potential application of this new class of substances as agrochemicals, here we present

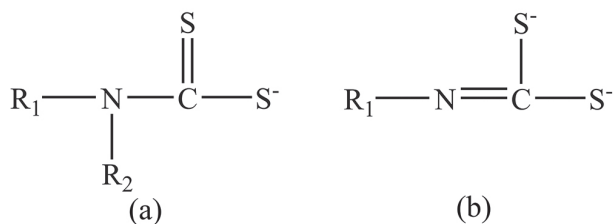


Figure 1. General formulae of dithiocarbamate (a) and dithiocarbimate (b) anions.

*e-mail: mayura@ufv.br

an extension of this research, with the syntheses of twelve new allyldithiocarbimate salts, now derived from aliphatic sulfonyldithiocarbimates and different MBH derivatives. The allyldithiocarbimate anions were isolated as tetraphenylphosphonium salts and were fully characterized by high-resolution electrospray ionization mass spectrometry (HR-ESI-MS), infrared and nuclear magnetic resonance (NMR) spectroscopies. X-ray diffraction experiments supported the proposed structures.

This work also presents a study on the activities of the allyldithiocarbimate salts against *Hemileia vastatrix* and *Phakopsora pachyrhizi*. Severe coffee leaf-rust epidemics have affected a number of countries, especially from Peru to Mexico, in the last decade, being the most important disease in the Brazilian coffee crops. The causal agent, *H. vastatrix*, is an obligate parasite and affects the aerial part of the plant, causing an early fall of leaves and drying of the branches, consequently reducing productivity.^{9,10} Asian soybean rust, caused by *P. pachyrhizi* is also a major problem in Brazil. Original from Asia, the fungus was first detected in 2001 in Paraguay, spreading within four years throughout the continent, up to the United States of America. Loss of sensibility of the fungus to available fungicides has already been reported.¹¹

Experimental

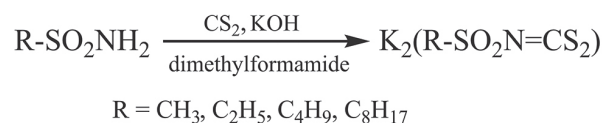
Methods and materials

Melting points (mp) were determined with an MQAPF-302 equipment (Microquímica) and are reported without correction. High resolution mass spectra (HRMS) were recorded on a micrOTOF Q-II liquid chromatography mass spectrometer (UltraflexIII, Bruker Daltonics) under electrospray ionization (ESI). Infrared (IR) spectra were recorded on a Varian 660-IR, equipped with GladiATR (attenuated total reflection, ATR) scanning from 4000 to 500 cm^{-1} . The ^1H and ^{13}C NMR spectra were recorded on a Varian Mercury 300 instrument (300 and 75 MHz, respectively), using deuterated chloroform as solvent and tetramethylsilane (TMS) as internal standard. Nuclear Overhauser effect spectroscopy (NOESY) experiments were

performed for structural characterization of the reaction products. Thin layer chromatography (TLC) analysis was conducted on aluminum precoated silica gel plates. Carbon disulfide, potassium hydroxide, ammonia aqueous solution, dimethyl sulfoxide and dimethylformamide were purchased from Vetec (Duque de Caxias, Brazil). The remaining reagents were purchased from Sigma-Aldrich (St. Louis, USA) and were used without further purification.

Syntheses of the precursors

The potassium *N*-R-sulfonyldithiocarbimates were prepared by the reaction of the appropriated sulfonamides with carbon disulfide and two molar equivalents of potassium hydroxide in dimethylformamide (Scheme 1), as described in the literature.¹²⁻¹⁴ The potassium dithiocarbimates were characterized by infrared and NMR spectroscopies, in comparison with reported data.¹²⁻¹⁴

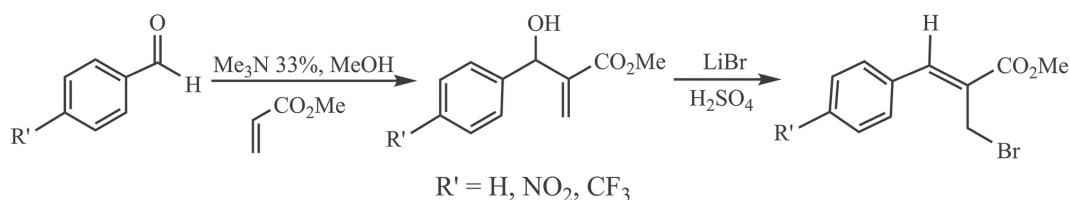


Scheme 1. Preparation of potassium *N*-R-sulfonyldithiocarbimates.

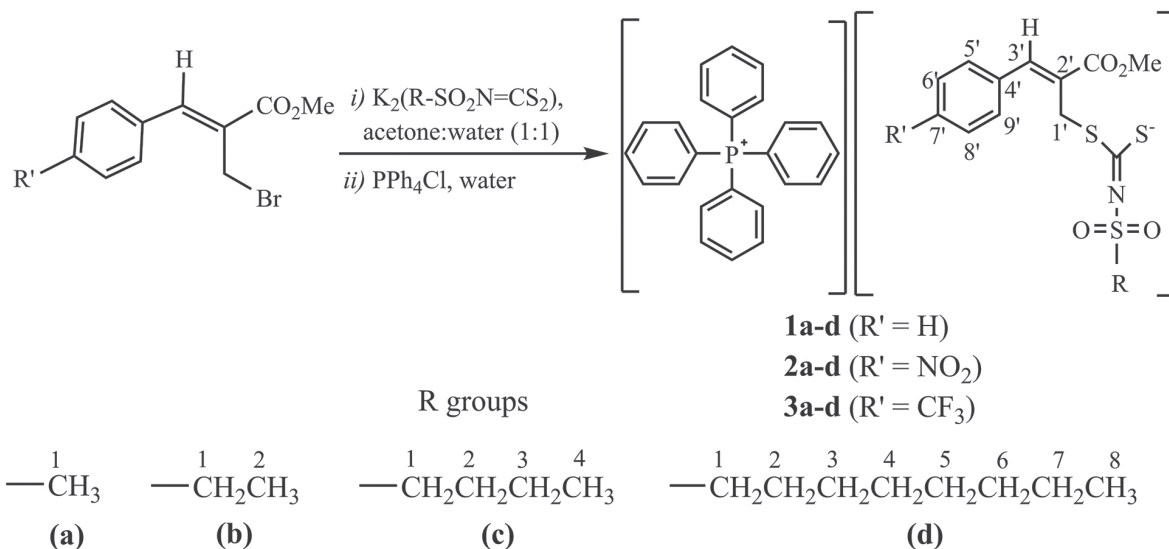
Three MBH adducts (Scheme 2) were prepared by the reaction of methyl acrylate with benzaldehyde, 4-nitrobenzaldehyde or 4-(trifluoromethyl)benzaldehyde, catalyzed by trimethylamine,¹⁵ and were converted into the respective allylic bromides (Scheme 2), in reaction with lithium bromide and sulfuric acid, as described in the literature.^{16,17} The allylic bromides were characterized by infrared and NMR spectroscopies, in comparison with reported data.^{16,17}

Syntheses of the allyldithiocarbimates (**1a-d**, **2a-d** and **3a-d**)

A solution of 1 mmol of each allylic bromide in acetone (2 mL) was added dropwise to a stirring acetone:water (1:1 by volume) solution (10 mL) containing 1.2 mmol of the appropriate potassium *N*-R-sulfonyldithiocarbimate (Scheme 3). The mixture was stirred for up to 15 min (monitored by TLC) at room temperature. Then, water



Scheme 2. Preparation of the Morita-Baylis-Hillman derivatives.



Scheme 3. Syntheses of the allyldithiocarbimates and numbering for NMR attribution.

(5 mL) was added and the product was extracted with ethyl acetate (3 × 20 mL).

For the syntheses of compounds **1a-c**, **2a-c** and **3a-c**, the organic phase was concentrated under reduced pressure and the residue was dissolved in water. Tetraphenylphosphonium chloride (1 mmol) was added and the mixture was stirred for 5 min. The yellow solid thus formed was filtered, washed with distilled water and dried under reduced pressure for one day. As compounds **1d**, **2d** and **3d** are oils, in these cases tetraphenylphosphonium chloride (1 mmol) was added directly to the organic phase (ethyl acetate). The mixture was stirred for 5 min. Then the organic solution was washed with water (2 × 20 mL), the organic solvent was evaporated, and the residue was dried under reduced pressure for one day.

The HRMS spectra of the products (**1a-d**, **2a-d**, **3a-d**) presented one peak at m/z 339.1318, in the positive mode, due to the tetraphenylphosphonium cation. Their NMR spectra showed the expected signals for the tetraphenylphosphonium cation at: ¹H NMR (300 MHz, CDCl₃) δ 7.50-7.68 (m*, 8H), 7.70-7.81 (m*, 8H), 7.85-7.93 (m, 4H) (*superimposed on the signals of H3', H5' and H9' of the anions); ¹³C NMR (75 MHz, CDCl₃) δ 117.5 (d, ¹J_{C-P} 90 Hz), 130.8 (d, ²J_{C-P} 7.5 Hz), 134.4 (d, ³J_{C-P} 7.5 Hz), 135.8 (d, ⁴J_{C-P} 3.0 Hz). The remaining signals and other experimental data are as follows.

Tetraphenylphosphonium (Z)-2-(methoxycarbonyl)-3-phenylallyl-(N-methylsulfonyl)dithiocarbamate (1a)

Yield 80%; mp 117.3-118.9 °C; IR (selected bands, ATR) ν / cm⁻¹ 1697 (ν C=O), 1373 (ν C=N), 1269 (ν _{as}SO₂), 1140 (ν _{sym}SO₂), 924 (ν _{as}CS₂); ¹H NMR (allyldithiocarbamate signals, 300 MHz, CDCl₃) δ 3.23 (s, 3H, H1), 3.72 (s,

3H, OCH₃), 4.20 (s, 2H, H1'), 7.22-7.37 (m, 3H, H6', H7', H8'), 7.49-7.97 (m*, 3H, H3', H5', H9'); ¹³C NMR (allyldithiocarbamate signals, 75 MHz, CDCl₃) δ 33.3 (C1'), 39.0 (C1), 52.1 (OCH₃), 127.3 (C2'), 128.6 (C6' and C8'), 128.8 (C7'), 130.1 (C5' and C9'), 134.8 (C4'), 141.3 (C3'), 168.3 (C=O), 201.6 (C=N); HRMS (ESI) m/z , calcd. for C₁₃H₁₄NO₄S₃⁻: 344.0090, found: 344.0107.

Tetraphenylphosphonium (Z)-2-(methoxycarbonyl)-3-phenylallyl-(N-ethylsulfonyl)dithiocarbamate (1b)

Yield 82%; mp 114.5-116.2 °C; IR (selected bands, ATR) ν / cm⁻¹ 1697 (ν C=O), 1365 (ν C=N), 1257 (ν _{as}SO₂), 1142 (ν _{sym}SO₂), 930 (ν _{as}CS₂); ¹H NMR (allyldithiocarbamate signals, 300 MHz, CDCl₃) δ 1.28 (t, 3H, *J* 7.5 Hz, H2), 3.46 (q, 2H, *J* 7.5 Hz, H1), 3.74 (s, 3H, OCH₃), 4.18 (s, 2H, H1'), 7.27-7.37 (m, 3H, H6', H7', H8'), 7.47-7.95 (m*, 3H, H3', H5', H9'); ¹³C NMR (allyldithiocarbamate signals, 75 MHz, CDCl₃) δ 8.4 (C2), 33.4 (C1'), 45.8 (C1), 52.3 (OCH₃), 127.3 (C2'), 128.6 (C6' and C8'), 128.9 (C7'), 130.1 (C5' and C9'), 134.8 (C4'), 141.5 (C3'), 168.3 (C=O), 201.6 (C=N); HRMS (ESI) m/z , calcd. for C₁₄H₁₆NO₄S₃⁻: 358.0247, found: 358.0240.

Tetraphenylphosphonium (Z)-2-(methoxycarbonyl)-3-phenylallyl-(N-butylsulfonyl)dithiocarbamate (1c)

Yield 75%; mp 91.6-92.4 °C; IR (selected bands, ATR) ν / cm⁻¹ 1705 (ν C=O), 1381 (ν C=N), 1261 (ν _{as}SO₂), 1147 (ν _{sym}SO₂), 933 (ν _{as}CS₂); ¹H NMR (allyldithiocarbamate signals, 300 MHz, CDCl₃) δ 0.83 (t, 3H, *J* 7.5 Hz, H4), 1.34 (sext, 2H, *J* 7.5 Hz, H3), 1.70-1.82 (m, 2H, H2), 3.51 (t, 2H, *J* 7.9 Hz, H1), 3.69 (s, 3H, OCH₃), 4.15 (s, 2H, H1'), 7.18-7.30 (m, 3H, H6', H7', H8'), 7.50-7.68 (m*, 3H, H3', H5', H9'), 7.47-7.63 (m, 3H, H3', H5', H9');

^{13}C NMR (allyldithiocarbamate signals, 75 MHz, CDCl_3) δ 13.9 (C4), 22.0 (C3), 25.7 (C2), 33.3 (C1'), 50.9 (C1), 52.1 (OCH_3), 127.3 (C2'), 128.6 (C6' and C8'), 128.8 (C7'), 130.2 (C5' and C9'), 134.8 (C4'), 141.3 (C3'), 168.3 (C=O), 200.8 (C=N); HRMS (ESI) m/z , calcd. for $\text{C}_{16}\text{H}_{20}\text{NO}_4\text{S}_3^-$: 386.0560, found: 386.0564.

Tetraphenylphosphonium (*Z*)-2-(methoxycarbonyl)-3-phenylallyl-(*N*-octylsulfonyl)dithiocarbamate (**1d**)

Yield 72%; oil at room temperature; IR (selected bands, ATR) ν / cm^{-1} 1705 ($\nu\text{C=O}$), 1381 ($\nu\text{C=N}$), 1259 ($\nu_{\text{as}}\text{SO}_2$), 1147 ($\nu_{\text{sym}}\text{SO}_2$), 933 ($\nu_{\text{as}}\text{CS}_2$); ^1H NMR (allyldithiocarbamate signals, 300 MHz, CDCl_3) δ 0.78-0.88 (m, 3H, H8), 1.17-1.42 (m, 10H, H3-H7), 1.74-1.89 (m, 2H, H2), 3.53 (t, 2H, J 8.1 Hz, H1), 3.72 (s, 3H, OCH_3), 4.19 (s, 2H, H1'), 7.19-7.35 (m, 3H, H6', H7', H8'), 7.50-7.68 (m*, 3H, H3', H5', H9'); ^{13}C NMR (allyldithiocarbamate signals, 75 MHz, CDCl_3) δ 14.2 (C8), 22.7 (C7), 23.7 (C6), 28.9 (C5), 29.2 (C4), 29.4 (C3), 31.9 (C2), 33.4 (C1'), 51.3 (C1), 52.1 (OCH_3), 127.4 (C2'), 128.6 (C6' and C8'), 128.8 (C7'), 130.2 (C5' and C9'), 134.9 (C4'), 141.2 (C3'), 168.3 (C=O), 200.8 (C=N); HRMS (ESI) m/z , calcd. for $\text{C}_{20}\text{H}_{28}\text{NO}_4\text{S}_3^-$: 442.1186, found: 442.1106.

Tetraphenylphosphonium (*Z*)-2-(methoxycarbonyl)-3-(4-nitrophenyl)allyl-(*N*-methylsulfonyl)dithiocarbamate (**2a**)

Yield 78%; mp 147.8-149.5 °C; IR (selected bands, ATR) ν / cm^{-1} 1720 ($\nu\text{C=O}$), 1510 ($\nu_{\text{as}}\text{NO}_2$), 1440 ($\nu_{\text{sym}}\text{NO}_2$), 1388 ($\nu\text{C=N}$), 1262 ($\nu_{\text{as}}\text{SO}_2$), 1156 ($\nu_{\text{sym}}\text{SO}_2$), 940 ($\nu_{\text{as}}\text{CS}_2$); ^1H NMR (allyldithiocarbamate signals, 300 MHz, CDCl_3) δ 3.25 (s, 3H, H1), 3.79 (s, 3H, OCH_3), 4.21 (s, 2H, H1'), 7.69-7.71 (m*, 1H, H3'), 7.73-7.84 (m*, 2H, H5', H9'), 8.15 (d, 2H, J 8.1 Hz, H6', H8'); ^{13}C NMR (allyldithiocarbamate signals, 75 MHz, CDCl_3) δ 32.9 (C1'), 38.9 (C1), 52.4 (OCH_3), 123.7 (C6' and C8'), 131.5 (C3'), 132.0 (C2'), 137.9 (C5' and C9'), 141.4 (C4'), 147.3 (C7'), 167.6 (C=O), 200.7 (C=N); HRMS (ESI) m/z , calcd. for $\text{C}_{13}\text{H}_{13}\text{N}_2\text{O}_6\text{S}_3^-$: 388.9941, found: 388.9944.

Tetraphenylphosphonium (*Z*)-2-(methoxycarbonyl)-3-(4-nitrophenyl)allyl-(*N*-ethylsulfonyl)dithiocarbamate (**2b**)

Yield 84%; mp 127.8-129.2 °C; IR (selected bands, ATR) ν / cm^{-1} 1711 ($\nu\text{C=O}$), 1518 ($\nu_{\text{as}}\text{NO}_2$), 1381 ($\nu\text{C=N}$), 1338 ($\nu_{\text{sym}}\text{NO}_2$), 1259 ($\nu_{\text{as}}\text{SO}_2$), 1144 ($\nu_{\text{sym}}\text{SO}_2$), 931 ($\nu_{\text{as}}\text{CS}_2$); ^1H NMR (allyldithiocarbamate signals, 300 MHz, CDCl_3) δ 1.26 (t, 3H, J 7.5 Hz, H2), 3.53 (q, 2H, J 7.5 Hz, H1), 3.75 (s, 3H, OCH_3), 4.18 (s, 2H, H1'), 7.54-7.64 (m*, 1H, H3'), 7.69-7.83 (m*, 2H, H5', H9'), 8.12 (d, 2H, J 8.7 Hz, H6', H8'); ^{13}C NMR (allyldithiocarbamate signals, 75 MHz, CDCl_3) δ 8.4 (C2), 33.0 (C1'), 45.3 (C1), 52.4 (OCH_3), 123.7 (C6' and C8'), 130.9 (C3'), 131.5 (C2'), 137.8

(C5' and C9'), 141.4 (C4'), 147.3 (C7'), 167.6 (C=O), 200.1 (C=N); HRMS (ESI) m/z , calcd. for $\text{C}_{14}\text{H}_{15}\text{N}_2\text{O}_6\text{S}_3^-$: 403.0098, found: 403.0043.

Tetraphenylphosphonium (*Z*)-2-(methoxycarbonyl)-3-(4-nitrophenyl)allyl-(*N*-butylsulfonyl)dithiocarbamate (**2c**)

Yield 80%; mp 120.7-122.6 °C; IR (selected bands, ATR) ν / cm^{-1} 1703 ($\nu\text{C=O}$), 1512 ($\nu_{\text{as}}\text{NO}_2$), 1392 ($\nu\text{C=N}$), 1342 ($\nu_{\text{sym}}\text{NO}_2$), 1255 ($\nu_{\text{as}}\text{SO}_2$), 1146 ($\nu_{\text{sym}}\text{SO}_2$), 928 ($\nu_{\text{as}}\text{CS}_2$); ^1H NMR (allyldithiocarbamate signals, 300 MHz, CDCl_3) δ 0.87 (t, 3H, J 7.5 Hz, H4), 1.38 (sext, 2H, J 7.5 Hz, H3), 1.73-1.84 (m, 2H, H2), 3.56 (t, 2H, J 7.8 Hz, H1), 3.78 (s, 3H, OCH_3), 4.21 (s, 2H, H1'), 7.57-7.69 (m*, 1H, H3'), 7.72-7.83 (m*, 2H, H5', H9'), 8.15 (d, 2H, J 8.7 Hz, H6', H8'); ^{13}C NMR (allyldithiocarbamate signals, 75 MHz, CDCl_3) δ 13.9 (C4), 22.0 (C3), 25.8 (C2), 33.0 (C1'), 50.9 (C1), 52.5 (OCH_3), 123.8 (C6' and C8'), 131.0 (C3'), 131.6 (C2'), 137.8 (C5' and C9'), 141.5 (C4'), 147.4 (C7'), 167.7 (C=O), 200.0 (C=N); HRMS (ESI) m/z , calcd. for $\text{C}_{14}\text{H}_{15}\text{N}_2\text{O}_6\text{S}_3^-$: 431.0411, found: 431.0388.

Tetraphenylphosphonium (*Z*)-2-(methoxycarbonyl)-3-(4-nitrophenyl)allyl-(*N*-butylsulfonyl)dithiocarbamate (**2d**)

Yield 75%; oil at room temperature; IR (selected bands, ATR) ν / cm^{-1} 1711 ($\nu\text{C=O}$), 1516 ($\nu_{\text{as}}\text{NO}_2$), 1381 ($\nu\text{C=N}$), 1342 ($\nu_{\text{sym}}\text{NO}_2$), 1259 ($\nu_{\text{as}}\text{SO}_2$), 1147 ($\nu_{\text{sym}}\text{SO}_2$), 935 ($\nu_{\text{as}}\text{CS}_2$); ^1H NMR (allyldithiocarbamate signals, 300 MHz, CDCl_3) δ 0.78-0.93 (m, 3H, H8), 1.14-1.47 (m, 10H, H3-H7), 1.70-1.85 (m, 2H, H2), 3.52 (t, 2H, J 8.1 Hz, H1), 3.79 (s, 3H, OCH_3), 4.20 (s, 2H, H1'), 7.56-7.70 (m*, 1H, H3'), 7.71-7.83 (m*, 2H, H5', H9'), 8.17 (d, 2H, J 8.7 Hz, H6', H8'); ^{13}C NMR (allyldithiocarbamate signals, 75 MHz, CDCl_3) δ 14.1 (C8), 22.6 (C7), 23.7 (C6), 28.8 (C5), 29.1 (C4), 29.3 (C3), 31.8 (C2), 33.0 (C1'), 51.4 (C1), 52.5 (OCH_3), 123.8 (C6' and C8'), 131.0 (C3'), 131.5 (C2'), 137.8 (C5' and C9'), 141.4 (C4'), 147.3 (C7'), 167.6 (C=O), 200.0 (C=N); HRMS (ESI) m/z , calcd. for $\text{C}_{20}\text{H}_{27}\text{N}_2\text{O}_6\text{S}_3^-$: 487.1037, found: 487.0995.

Tetraphenylphosphonium (*Z*)-2-(methoxycarbonyl)-3-[4-(trifluoromethyl)phenyl]allyl-(*N*-methylsulfonyl)dithiocarbamate (**3a**)

Yield 89%; mp 136.8-138.5 °C; IR (selected bands, ATR) ν / cm^{-1} 1722 ($\nu\text{C=O}$), 1385 ($\nu\text{C=N}$), 1261 ($\nu_{\text{as}}\text{SO}_2$), 1151 ($\nu_{\text{sym}}\text{SO}_2$), 1063 (νCF_3), 930 ($\nu_{\text{as}}\text{CS}_2$); ^1H NMR (allyldithiocarbamate signals, 300 MHz, CDCl_3) δ 3.21 (s, 3H, H1), 3.75 (s, 3H, OCH_3), 4.17 (s, 2H, H1'), 7.52-7.69 (m*, 5H, H3', H5', H6', H8', H9'); ^{13}C NMR (allyldithiocarbamate signals, 75 MHz, CDCl_3) δ 33.2 (C1'), 39.1 (C1), 52.4 (OCH_3), 125.5 (q, J 3.7 Hz, C6' and C8'), 127.7 (q, J 270 Hz, CF_3), 129.9 (C2'), 130.3 (C5' and

C9'), 130.6 (q, J 32 Hz, C7'), 138.4 (C3'), 139.3 (C4'), 167.9 (C=O), 201.3 (C=N); HRMS (ESI) m/z , calcd. for $C_{14}H_{13}F_3NO_4S_3^-$: 411.9964, found: 411.9961.

Tetraphenylphosphonium (*Z*)-2-(methoxycarbonyl)-3-[4-(trifluoromethyl)phenyl]allyl-(*N*-ethylsulfonyl) dithiocarbamate (**3b**)

Yield 85%; mp 133.8-135.2 °C; IR (selected bands, ATR) ν / cm^{-1} 1718 ($\nu_{\text{C=O}}$), 1379 ($\nu_{\text{C=N}}$), 1261 ($\nu_{\text{as}}\text{SO}_2$), 1153 ($\nu_{\text{sym}}\text{SO}_2$), 1061 (ν_{CF_3}), 930 ($\nu_{\text{as}}\text{CS}_2$); ^1H NMR (allyldithiocarbamate signals, 300 MHz, CDCl_3) δ 1.29 (t, 3H, J 7.5 Hz, H2), 3.54 (q, 2H, J 7.5 Hz, H1), 3.76 (s, 3H, OCH_3), 4.19 (s, 2H, H1'), 7.54-7.70 (m*, 5H, H3', H5', H6', H8', H9'); ^{13}C NMR (allyldithiocarbamate signals, 75 MHz, CDCl_3) δ 8.4 (C2), 33.1 (C1'), 45.4 (C1), 52.3 (OCH_3), 125.5 (q, J 3.8 Hz, C6' and C8'), 127.6 (q, J 270 Hz, CF_3), 129.9 (C2'), 130.3 (C5' and C9'), 130.5 (q, J 31.5 Hz, C7'), 138.4 (C3'), 139.0 (C4'), 167.9 (C=O), 200.3 (C=N); HRMS (ESI) m/z , calcd. for $C_{15}H_{15}F_3NO_4S_3^-$: 426.0121, found: 426.0142.

Tetraphenylphosphonium (*Z*)-2-(methoxycarbonyl)-3-[4-(trifluoromethyl)phenyl]allyl-(*N*-butylsulfonyl) dithiocarbamate (**3c**)

Yield 79%; mp 119.2-120.8 °C; IR (selected bands, ATR) ν / cm^{-1} 1705 ($\nu_{\text{C=O}}$), 1396 ($\nu_{\text{C=N}}$), 1255 ($\nu_{\text{as}}\text{SO}_2$), 1157 ($\nu_{\text{sym}}\text{SO}_2$), 1065 (ν_{CF_3}), 926 ($\nu_{\text{as}}\text{CS}_2$); ^1H NMR (allyldithiocarbamate signals, 300 MHz, CDCl_3) δ 0.86 (t, 3H, J 7.2 Hz, H4), 1.38 (sext, 2H, J 7.5 Hz, H3), 1.73-1.84 (m, 2H, H2), 3.54 (t, 2H, J 8.1 Hz, H1), 3.76 (s, 3H, OCH_3), 4.19 (s, 2H, H1'), 7.52-7.70 (m*, 5H, H3', H5', H6', H8', H9'); ^{13}C NMR (allyldithiocarbamate signals, 75 MHz, CDCl_3) δ 13.9 (C4), 22.0 (C3), 25.8 (C2), 33.1 (C1'), 51.0 (C1), 52.4 (OCH_3), 125.5 (q, J 3.8 Hz, C6' and C8'), 127.7 (q, J 270.0 Hz, CF_3), 129.9 (C2'), 130.0 (C5' and C9'), 130.5 (q, J 31.5 Hz, C7'), 138.4 (C3'), 139.1 (C4'), 167.9 (C=O), 200.3 (C=N); HRMS (ESI) m/z , calcd. for $C_{17}H_{19}F_3NO_4S_3^-$: 454.0434, found: 454.0408.

Tetraphenylphosphonium (*Z*)-2-(methoxycarbonyl)-3-[4-(trifluoromethyl)phenyl]allyl-(*N*-octylsulfonyl) dithiocarbamate (**3d**)

Yield 72%; oil at room temperature; IR (selected bands, ATR) ν / cm^{-1} 1711 ($\nu_{\text{C=O}}$), 1381 ($\nu_{\text{C=N}}$), 1259 ($\nu_{\text{as}}\text{SO}_2$), 1163 ($\nu_{\text{sym}}\text{SO}_2$), 1065 (ν_{CF_3}), 933 ($\nu_{\text{as}}\text{CS}_2$); ^1H NMR (allyldithiocarbamate signals, 300 MHz, CDCl_3) δ 0.79-0.93 (m, 3H, H8), 1.12-1.45 (m, 10H, H3-H7), 1.72-1.88 (m, 2H, H2), 3.53 (t, 2H, J 7.8 Hz, H1), 3.76 (s, 3H, OCH_3), 4.19 (s, 2H, H1'), 7.56-7.70 (m*, 5H, H3', H5', H6', H8', H9'); ^{13}C NMR (allyldithiocarbamate signals, 75 MHz, CDCl_3) δ 14.1 (C8), 22.6 (C7), 23.7 (C6), 28.8 (C5), 29.1 (C4),

29.3 (C3), 31.8 (C2), 33.0 (C1'), 51.3 (C1), 52.3 (OCH_3), 125.4 (q, J 3.7 Hz, C6' and C8'), 127.6 (q, J 271.0 Hz, CF_3), 129.4 (C2'), 130.3 (C5' and C9'), 130.5 (q, J 31.5 Hz, C7'), 138.3 (C3'), 139.0 (C4'), 167.8 (C=O), 200.2 (C=N); HRMS (ESI) m/z , calcd. for $C_{21}H_{27}F_3NO_4S_3^-$: 510.1060, found: 510.0993.

X-ray crystallography

Yellow crystals of the compound **2a** were obtained by slow evaporation of a dichloromethane/ethanol solution (1:1) and a few drops of water at 25 °C. The diffraction measurement was achieved at room temperature with a Bruker APEX II CCD diffractometer using Mo $K\alpha$ radiation (λ 0.71073 Å). Data collection, cell refinement and data reduction were made using APEX2 software.¹⁸ Final unit cell parameters based on all reflections were obtained by least squares refinement. The data were integrated via SAINT.¹⁹ Lorentz and polarization effect and multi-scan absorption corrections were applied with SADABS.²⁰ The structure was solved with SHELXS97 using direct methods and refined by full-matrix least-square methods against F^2 (SHELXL-2014).^{21,22} All hydrogen atoms were stereochemically positioned and refined with the riding model. The crystal structure was refined as a non-merohedral twin with a 2-fold axis rotation around the c^* axis (c -axis of the reciprocal space) and a BASF parameter of 0.04767. Structural representations were drawn using ORTEP-3²³ and MERCURY.²⁴ The program WinGX was used to prepare materials for publication.²³ The data collection and experimental details for compound **2a** can be found in the Table 1.

Biological assay

The culture medium, prepared with agar-agar (Vetec, Duque de Caxias, Brazil) and distilled water, was sterilized by autoclaving at 121 °C for 25 min. Each compound was dissolved in dimethyl sulfoxide and Tween 80 (0.75 mL each) and the solutions were homogeneously mixed with the agar-agar suspension (100 mL) and verted into sterile Petri dishes. The final concentrations for each tested substance in the culture medium were equal to 15, 30, 60, 120, 240, 360, 480 and 960 $\mu\text{mol L}^{-1}$. Each treatment had three replicates. The zinc bis-dimethyldithiocarbamate (97%, Sigma-Aldrich, St. Louis, USA) was included as a positive control in the tests at 120 $\mu\text{mol L}^{-1}$ and the results were compared by the Tukey's test ($p \leq 0.05$).

Phakopsora pachyrhizi and *Hemileia vastatrix* spores were isolated from infected soybean (*Glycine max*, cultivar: Monarca) and coffee (*Coffea arabica*, cultivar: Red

Table 1. Crystallographic data and details of diffraction experiments for compound **2a**

Empirical formula	C ₃₇ H ₃₃ NO ₆ PS ₃
Formula weight / (g mol ⁻¹)	728.80
Temperature / K	296(2)
Crystal system	monoclinic
Space group	P2 ₁ /c
Unit cell dimensions	
<i>a</i> / Å	7.808(1)
<i>b</i> / Å	14.182(1)
<i>c</i> / Å	32.506(2)
β / degree	93.209(2)
Volume / Å ³	3594.2(3)
Z	4
Calculated density / (g cm ⁻³)	1.347
μ / mm ⁻¹	0.299
T _{min} /T _{max}	0.902/0.926
F(000)	1520
Crystal size / mm	0.386 × 0.288 × 0.256
θ range / degree	0.627 to 26.403
Limiting indices	-5 ≤ <i>h</i> ≤ 9; -17 ≤ <i>k</i> ≤ 13; -40 ≤ <i>l</i> ≤ 38
Reflections collected	19122
Independent reflections	7358 [R(int) = 0.0365]
Goodness-of-fit	1.087
Data / restraints / parameters	5872 / 0 / 444
R indices [I > 2σ(I)]	R = 0.0853, wR = 0.2806
R indices (all data)	R = 0.1030, wR = 0.3057
Largest diff. peak and hole / (e Å ⁻³)	1.097 and -0.701

$$R = \frac{\sum (|F_o| - |F_c|)}{\sum |F_o|}; wR = \left[\frac{\sum w (|F_o^2| - |F_c^2|)}{\sum w |F_o^2|} \right]^{1/2}$$

μ: absorption coefficient; F(000): structure factor in the zeroth-order case; R(int): internal R-value.

Caturra) leaves, respectively. The spore concentrations were adjusted to 1×10^5 spore mL⁻¹ in distilled water, with the aid of a hemocytometer. Then, 100 μL of these suspensions were added to each Petri dish and homogeneously spread over the culture medium. After 24 h of incubation at 25 °C, each plate was divided into four quadrants and 25 spores *per* quadrant were examined under the microscope to assess germination. The averages were compared to the negative control (prepared using dimethyl sulfoxide, Tween 80 and agar-agar only) and the inhibition percentages were calculated. The results were statistically analyzed by nonlinear regression using the concentration logarithm *versus* percent inhibition results. The activities were submitted to analyses of variance. The needed concentrations to achieve 50 and 90% of inhibition

of spore germination (IC₅₀ and IC₉₀ values) were calculated for each compound from the regression equations.^{25,26} The whole experiment was repeated, and the results confirmed the first data set (see Tables S1, S2 and S3 in the Supplementary Information).

Results and Discussion

Syntheses and characterization

Twelve novel allyldithiocarbamate anions were prepared by the reactions between aliphatic sulfonyldithiocarbimates and allylic bromides derived from MBH adducts (Scheme 3). There is only one paper⁸ in the literature reporting the synthesis of allyldithiocarbimates, though these were derived from aromatic sulfonyldithiocarbimates. Using a similar approach, here we demonstrate that the aliphatic sulfonyldithiocarbimates also act as nucleophiles, reacting in a fast way with the allylic bromides at room temperature (less than 15 min) furnishing the allyldithiocarbimates in good yields (72-82%).

As the resulting potassium salts are water soluble and not easily purifiable, the new compounds were isolated as tetraphenylphosphonium salts. The new salts are yellow solids (**1a-c**, **2a-c** and **3a-c**) or yellowish viscous oils (**1d**, **2d** and **3d**) at room temperature, soluble in dimethyl sulfoxide, dimethylformamide, acetone, ethyl acetate, ethanol, chloroform and dichloromethane, with very low solubility in diethyl ether, hexanes and water. Their molecular formulae were confirmed by HRMS, which presented the expected peak for the tetraphenylphosphonium ion in the positive mode, and the molecular ion peaks of each allyldithiocarbamate in the negative mode. The ¹H NMR spectra integration curves were in accordance with a 1:1 proportion between each anion and the tetraphenylphosphonium cation.

Characteristic bands in the IR spectra indicated the presence of the most relevant groups within each structure. All spectra presented the α,β-unsaturated ester carbonyl band at around 1710 cm⁻¹, the C=N and CS₂ stretching bands at ca. 1380 and 930 cm⁻¹, respectively, and the strong bands due to the SO₂ group at ca. 1260 and 1150 cm⁻¹. The C=N bands were shifted to higher wavenumber values with respect to the parent potassium dithiocarbimates data (νCN 1260-1300 cm⁻¹).¹²⁻¹⁴ This shift can be explained by the partial loss of conjugation within the NCS₂ system. Consequently, the CS₂ bands had the opposite shift (potassium dithiocarbimates νCS₂ 945-979 cm⁻¹). Compounds **2a-d** and **3a-d** IR spectra presented additional bands due to the nitro (ca. 1515 and 1340 cm⁻¹) and trifluoromethyl (ca. 1065 cm⁻¹) groups.

The signals due to the alkyl groups in the ^{13}C NMR spectra had similar chemical shift values when compared to the parent potassium dithiocarbimates.¹²⁻¹⁴ One important change was observed on the signal of the carbon atom of the NCS_2 group, which was shifted from ca. δ 224 in the spectra of the precursors to ca. δ 200 in the spectra of the allyldithiocarbimates. This shift is in agreement with the IR data, and is due to the greater double bond character of the CN bond in the allyldithiocarbimates. Two signals in higher field (ca. δ 33 and 52), present in all spectra, were due to the CH_2 and OCH_3 carbon atoms of the MBH moiety, and the ester carbonyl signal was observed at ca. δ 168. The spectra of compounds **3a-d** showed a quartet centered at ca. δ 128 (J 270 Hz) due to the CF_3 group, which also caused the split in the aromatic signals at around δ 130.5 (2J 31.5 Hz, $\text{C}7'$) and δ 125.5 (3J 3.8 Hz, $\text{C}6'$ and $\text{C}8'$).

In order to investigate the stereochemistry of the allyldithiocarbimates, NOESY experiments were performed. A correlation between the hydrogens $\text{H}1'$ and $\text{H}9'$ signals indicated a spatial proximity coherent with a *Z* configuration with respect to the $\text{C}2'-\text{C}3'$ double bond.

X-ray crystallography

Compound **2a** crystallizes in the monoclinic space group $\text{P}2_1/c$. The asymmetric unit contains one anion and one cation (Figure 2). Single crystal X-ray diffraction data confirmed the (*Z*)-stereochemistry for the allyldithiocarbimate anion.

Selected bond lengths and torsion angles are summarized in Table 2. The bond length $\text{C}2'-\text{C}3'$ [1.329(8) Å] is consistent with a normal $\text{C}=\text{C}$ double bond (1.34 Å). The

Table 2. Selected bond lengths and torsion angles for compound **2a**

Bond length / Å	
S1–C1	1.735(7)
S1–N1	1.623(5)
C2–N1	1.306(7)
C2–S3	1.689(5)
C2–S2	1.777(5)
S2–C1'	1.830(6)
C1'–C2'	1.515(7)
C2'–C3'	1.329(8)
C3'–C4'	1.464(9)
C2'–C3	1.506(8)
C3–O4	1.341(8)
C3–O3	1.191(8)
O4–C4	1.453(9)
C7'–N1	1.469(9)
Torsion angle / degree	
C2–S2–C1'–C2'	111.66
S2–C1'–C2'–C3'	–121.15
S2–C1'–C2'–C3	60.92

$\text{C}2'-\text{C}3$ bond [1.506(8) Å] is in the range of a $\text{Csp}^2\text{-Csp}^3$ sigma bond (1.50 Å). The bond lengths (Table 2) within the methoxycarbonyl group ($\text{C}3-\text{O}3$, $\text{C}3-\text{O}4$ and $\text{C}4-\text{O}4$) are within the range reported for the analogues derived from aromatic sulfonildithiocarbimates.⁸ The $\text{N}1-\text{C}2$ bond distance [1.306(7) Å] is slightly longer than the value of 1.279 Å for a typical $\text{N}(\text{sp}^2)=\text{C}(\text{sp}^2)$ double

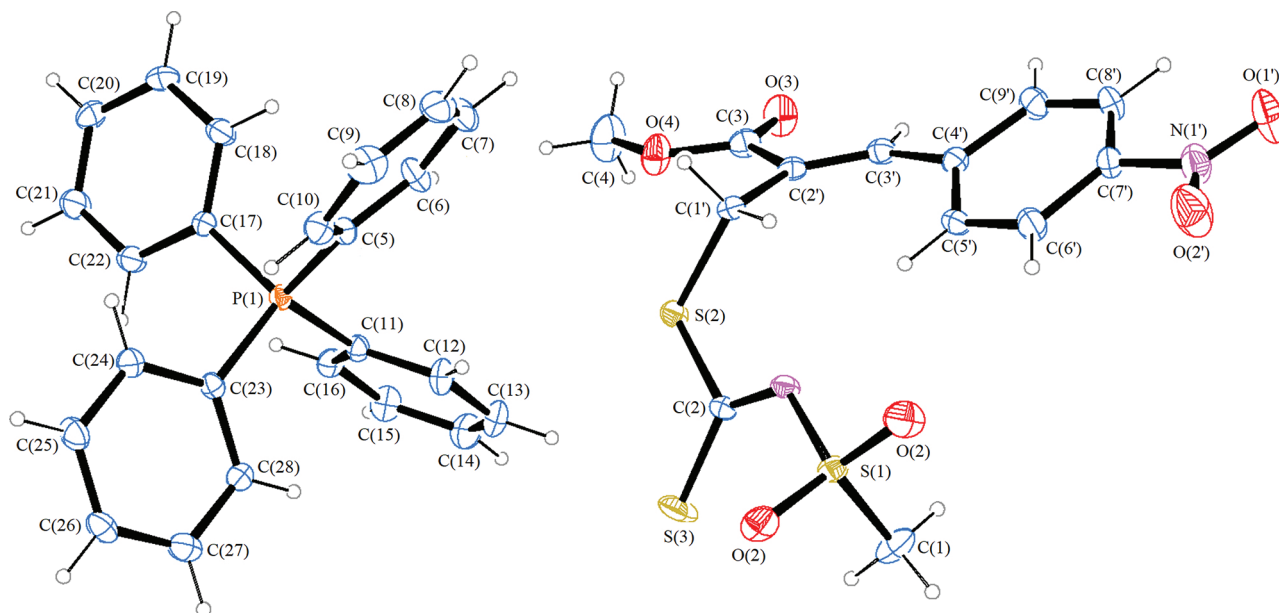


Figure 2. ORTEP view of compound **2a** with atom-numbering scheme and displacement ellipsoids drawn with 20% probability level, and numbering for the X-ray data analyses.

bond.²⁷ In addition, the C2–S2 bond length [1.777(5) Å] is significantly longer than the C2–S3 distance [1.689(5) Å]. The C2–S2 distance is shorter than a C–S single bond and the C2–S3 is slightly longer than a typical C=S double bond.²⁷ These facts are due to the conjugated NCS₂ system and agree with the IR and NMR data.

Three planar fragments characterize the anion: S1/N1/C2/S2/S3/C1', C2'/C3/O3/O4/C4/C1' and the phenyl ring. The angle between the first two fragments is 63.7(2)° and between the second and third fragments is 25.5(3)°. The torsion angles around the bonds C1'–C2' and S2–C1' describe the orientation of these fragments (Table 2).

The phosphorus atom in the tetraphenylphosphonium cation present tetrahedral distorted geometry, with P–C and C–C bond lengths in the range from 1.787(6) to 1.797(5) Å and 1.360(10) to 1.408(8) Å, respectively. The C–P–C angles in the four phenyl rings go from 107.4(2)

to 111.5(3)°. These values are comparable to those found in other structures with the same cation.^{8,28}

The crystal packing is mainly stabilized by the electrostatic interactions between oppositely charged ions (Figure 3). In addition, there are four intramolecular contacts in the anion, and intermolecular interactions between cations and anions (C–H...O), between anions (C–H...S) and between cations (C–H...Cg) (Table 3). The C16–H16...O1, C20–H20...O2 and C1'–H1'1...S3 intermolecular interactions form ribbons in the *a*-axis direction (Figure 3). The C25–H25...Cg interactions connect these ribbons forming chains along *b*-axis.

Antifungal activity

The influences of the twelve allyldithiocarbamate salts shown in Scheme 3 were investigated, *in vitro*, on the

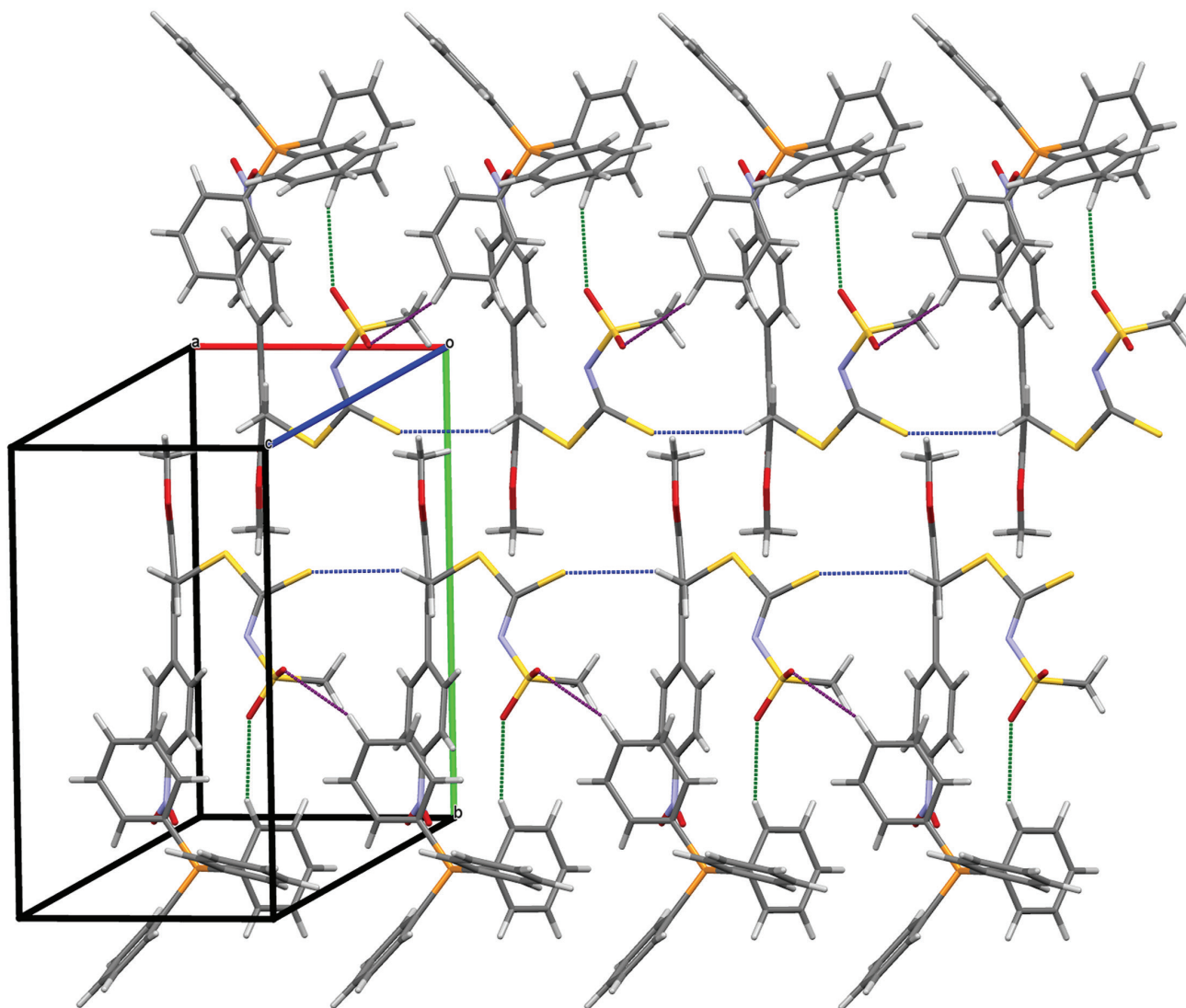


Figure 3. Structural packing of compound **2a** in the *a*-axis direction. Dashed lines indicate C16–H16...O1, C20–H20...O2 and C1'–H1'1...S3 hydrogen bonds.

Table 3. Geometric parameters for intramolecular and intermolecular interactions in compound **2a** crystal

Donor–H...acceptor	d(D–H) / Å	d(H...A) / Å	d(D...A) / Å	<(DHA) / degree
C1–H1A...S3	0.96	2.78	3.419(9)	125
C1'–H1'2...N1	0.97	2.40	2.940(7)	115
C3'–H3'...O3	0.93	2.33	2.759(8)	108
C5'–H5'...N1	0.93	2.42	3.345(8)	173
C16–H16...O1 ⁱ	0.93	2.56	3.423(7)	154
C20–H20...O2 ⁱⁱ	0.93	2.56	3.421(9)	155
C1'–H1'1...S3 ⁱⁱⁱ	0.97	2.86	3.675(6)	143
C25–H25...Cg ^{iv}	0.93	2.89	3.685(8)	144

Symmetry codes: (i) $x, 1 + y, z$; (ii) $-1 + x, 1 + y, z$; (iii) $-1 + x, y, z$; (iv) $1 - x, \frac{1}{2} + y, \frac{1}{2} - z$. Cg is the C23–C28 ring.

germination of *H. vastatrix* and *P. pachyrhizi* spores. The new compounds showed comparable activities to those presented by the ZDMC, the pure active principle of the protectant fungicide Ziram at $120 \mu\text{mol L}^{-1}$ (Figures 4 and 5). ZDMC and the new allyldithiocarbamate salts were more active against *P. pachyrhizi* than against *H. vastatrix*. The results also indicated that the structural differences on the allyldithiocarbamate interfere with their activities (Figures 4 and 5).

The new compounds were tested at various concentrations ranging from 15 to $960 \mu\text{mol L}^{-1}$, reaching 100% of inhibition of the spore germination of both fungi below the higher concentration tested. The inhibition percentages were correlated to the logarithm of the allyldithiocarbamate salts concentrations, furnishing the curve equations shown in Tables 4 and 5. All equations presented coefficient of determination values (r^2) very close to 1.0. The F value and $\text{Prob} > F$ statistics were used to test

the overall significance of the regression model. The results showed that the choice of the sigmoidal dose-response model was adequate with a high level of significance ($\text{Prob} > F$ of less than 0.01). Figure 6 exemplifies the dose response curves obtained. In order to confirm the results, the whole experiment was repeated in different days. The data were reproducible as shown in Figure 6.

The necessary concentrations to inhibit 50 and 90% of spore germination (IC_{50} and IC_{90} values, respectively) were calculated from the equations shown in Tables 4 and 5. The results are listed in Table 6. The complete set of results confirmed that the new compounds are significantly more active against *P. pachyrhizi* than against *H. vastatrix*, both at lower and higher concentration ranges.

It is also clear that the molecular differences within the allyldithiocarbamate anions interfere on the activity, as the various combinations of R (**a-d**) and R' (**1-3**) groups lead to different results (Table 6). With respect to the alkyl

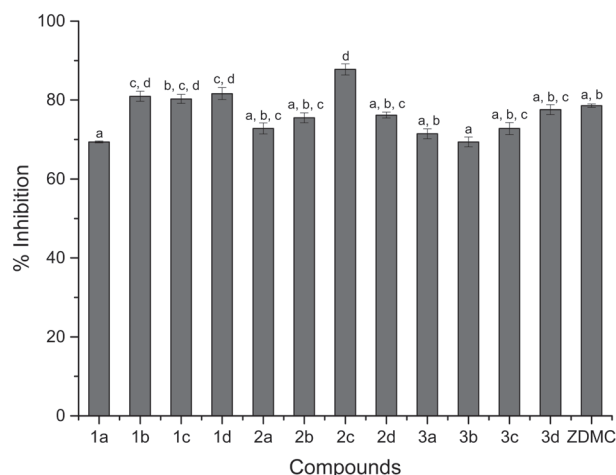


Figure 4. Inhibition (in percentage) of *P. pachyrhizi* spore germination caused by the new allyldithiocarbamate salts compared to the positive control, zinc bis-dimethyldithiocarbamate (ZDMC) at $120 \mu\text{mol L}^{-1}$. Values followed by the same letter do not differ at the 5% level of significance by the Tukey's test.

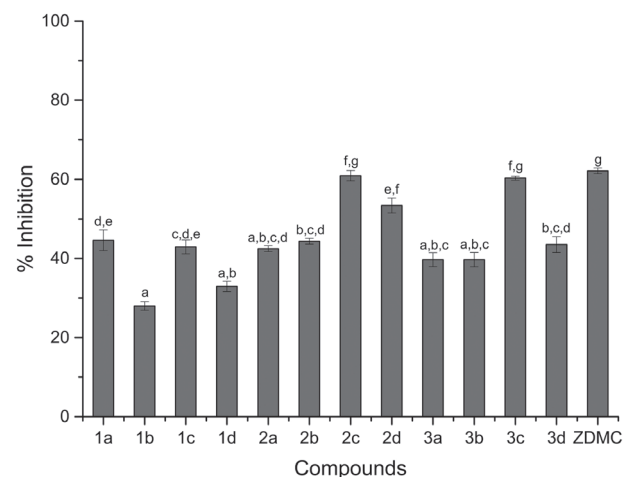


Figure 5. Inhibition (in percentage) of *H. vastatrix* spore germination caused by the new allyldithiocarbamate salts compared to the positive control, zinc bis-dimethyldithiocarbamate (ZDMC) at $120 \mu\text{mol L}^{-1}$. Values followed by the same letter do not differ at the 5% level of significance by the Tukey's test.

Table 4. Regression equation for the inhibition of *P. pachyrhizi* spore germination versus the log of the allyldithiocarbimate salts concentrations, equation parameters and statistical data

Compound	Equation: $y = A1 + \frac{(A2 - A1)}{(1 + 10^{(LOGx0 - x)p})}$				Statistical data		
	A1	A2	LOGx0	p	r ²	F	Prob > F
1a	13.08	100.74	-1.01	2.25	0.9822	442.89	< 0.0001
1b	10.91	99.08	-1.13	2.42	0.9921	1077.50	< 0.0001
1c	-503.64	112.63	-3.43	0.51	0.9819	1197.90	< 0.0001
1d	15.66	102.16	-1.38	1.21	0.9832	1299.22	< 0.0001
2a	22.03	101.43	-1.04	2.19	0.9936	1676.69	< 0.0001
2b	3.89	107.69	-1.23	0.99	0.9835	854.70	< 0.0001
2c	-3.30	101.53	-1.41	1.51	0.9954	2779.41	< 0.0001
2d	-4.65	100.29	-1.25	1.65	0.9921	1066.90	< 0.0001
3a	19.20	104.14	-1.05	1.43	0.9909	1391.44	< 0.0001
3b	15.03	108.62	-1.03	1.12	0.9873	1027.00	< 0.0001
3c	29.78	104.31	-1.03	1.53	0.9936	1667.36	< 0.0001
3d	1.90	105.51	-1.25	1.13	0.9864	939.17	< 0.0001

y: inhibition percentage; A1: bottom asymptote; A2: top asymptote; LOGx0: center; x: log₁₀[concentration]; p: hill slope; r²: coefficient of determination; F: value obtained by the F-test; Prob > F = probability value (p model, F < 0.0001).

Table 5. Regression equation for the inhibition of *H. vastatrix* spore germination versus the log of the allyldithiocarbimate salts concentrations, equation parameters and statistical data

Compound	Equation: $y = A1 + \frac{(A2 - A1)}{(1 + 10^{(LOGx0 - x)p})}$				Statistical data		
	A1	A2	LOGx0	p	r ²	F	Prob > F
1a	8.16	102.7	-0.84	2.43	0.9972	1986.84	< 0.0001
1b	5.48	100.62	-0.77	3.19	0.9949	895.97	< 0.0001
1c	11.67	103.61	-0.83	2.45	0.9911	680.87	< 0.0001
1d	11.13	106.39	-0.69	2.06	0.9849	371.58	< 0.0001
2a	15.85	102.11	-0.81	2.48	0.9831	394.85	< 0.0001
2b	10.00	118.30	-0.68	1.14	0.9772	337.11	< 0.0001
2c	23.60	103.21	-0.93	2.14	0.9904	1037.18	< 0.0001
2d	15.92	103.73	-0.90	2.18	0.9884	655.15	< 0.0001
3a	15.59	100.91	-0.79	2.69	0.9940	1070.26	< 0.0001
3b	9.53	116.12	-0.66	1.27	0.9760	283.56	< 0.0001
3c	20.38	103.98	-0.93	1.86	0.9931	1403.44	< 0.0001
3d	14.57	103.47	-0.81	2.34	0.9929	920.38	< 0.0001

y: inhibition percentage; A1: bottom asymptote; A2: top asymptote; LOGx0: center; x: log₁₀[concentration]; p: hill slope; r²: coefficient of determination; F: value obtained by the F-test; Prob > F = probability value (p model, F < 0.0001).

groups (**a-d**), the compounds with the butyl group (**c**) showed the best results within each series (**1a-d**, **2a-d** and **3a-d**), considering both the IC₅₀ and IC₉₀ values for *H. vastatrix* (Table 6). The same trend was observed for *P. pachyrhizi*, with one exception within the group **1a-d**. Membrane affinity follows a nonlinear behavior, usually increasing with the chain length up to a threshold, beyond

which lengthening of the chain results in a reduction on the biological activity.²⁹ The better performance of the compounds bearing the butyl group (**c**) points to an optimum chain length of ca. four carbon atoms for the inhibitory activity here studied.

The introduction of fluorine atoms and nitro groups in biologically active molecules is known to affect their

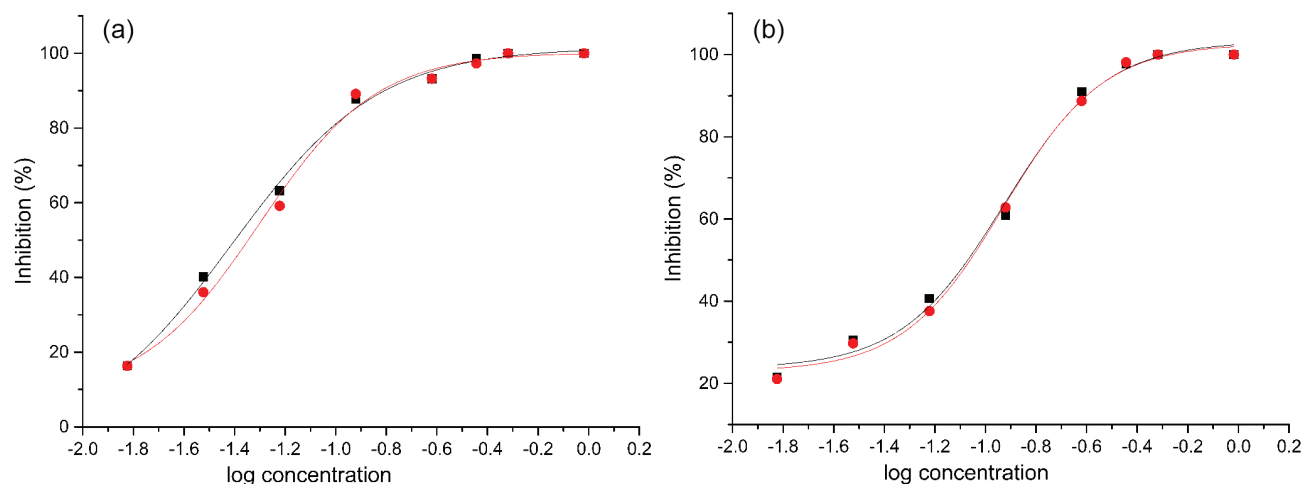


Figure 6. Dose-response curves for the inhibition (in percentage) of *P. pachyrhizi* (a) and *H. vastatrix* (b) spore germination by compound **2c** after 24 h of incubation at 25 °C, in two separate experiments, with three replicates *per* treatment in each experiment.

Table 6. Concentrations of the allyldithiocarbamate salts to inhibit 50% (IC₅₀) and 90% (IC₉₀) spore germination of *P. pachyrhizi* and *H. vastatrix*

Compound	Fungi			
	<i>P. pachyrhizi</i>		<i>H. vastatrix</i>	
	IC ₅₀ / ($\mu\text{mol L}^{-1}$)	IC ₉₀ / ($\mu\text{mol L}^{-1}$)	IC ₅₀ / ($\mu\text{mol L}^{-1}$)	IC ₉₀ / ($\mu\text{mol L}^{-1}$)
1a	85	234	130	308
1b	67	180	161	322
1c	26	223	129	302
1d	30	189	172	443
2a	69	205	132	320
2b	47	288	129	514
2c	40	156	85	252
2d	59	217	101	271
3a	60	274	142	334
3b	59	321	149	533
3c	49	240	84	275
3d	49	257	130	323

effectiveness. The presence of such substituents can alter important parameters such as interaction with enzymes, cell membranes and target receptors, or may produce secondary activity reactions, for example due to the enzymatic bio-reduction of nitro groups.³⁰⁻³³

Therefore, along with the compounds **1a-d** (with the unsubstituted phenyl ring), we included the analogues **2a-d** and **3a-d** in order to evaluate if the introduction of the nitro and trifluoromethyl substituents would affect the activity of the allyldithiocarbimates. The analysis of the results (Table 6) was not straightforward when considering the presence of these groups in the structures. The effect of both nitro (**2**) and trifluoromethyl (**3**) substituents on the IC₉₀ values are

positive for the inhibition of *H. vastatrix* when considering the analogues with the longer carbon chains (**c** and **d**). Nevertheless, these substituents lower the inhibition of *H. vastatrix* germination when the allyldithiocarbimates bear short alkyl groups (**a** and **b**). The results for *P. pachyrhizi* were even more complex with respect to the influence of the nitro group, while the trifluoromethyl group clearly diminishes the performance of these new antifungals.

Conclusions

The reactions between *N*-alkyl-sulfonyldithiocarbimates and allylic bromides are very fast and furnish allyldithiocarbimates in good yields. The X-ray diffraction studies confirmed that the reactions are stereospecific, furnishing exclusively the *Z* isomers, as the spectroscopic data also indicated.

The twelve new compounds inhibited the spore germination of *P. pachyrhizi* and *H. vastatrix* at very low doses. The activities were higher against *P. pachyrhizi*. It was observed that the alkyl chain with four carbon atoms increases the inhibitory activity in comparison with the homologues with one, two or eight carbon atoms, in most cases. The presence of the trifluorophenyl and nitro groups in the aromatic ring enhanced the activity of the allyldithiocarbimates against *H. vastatrix* for the compounds bearing the longer alkyl chains (**c** and **d**), showing opposite results for the shorter chains analogues (**a** and **b**). The influence of these groups seemed to be more complex with respect to *P. pachyrhizi*.

The best overall results were achieved in the treatments with compound **2c** (substituent on the aromatic ring = nitro; alkyl group = butyl), which resulted in the lowest IC₉₀ values (252 $\mu\text{mol L}^{-1}$ for *H. vastatrix*, and 156 $\mu\text{mol L}^{-1}$

for *P. pachyrhizi*). The experiments were repeated, and the results are reproducible. Considering the Tukey's test (Figure 4), the activity of compound **2c** on the germination of *P. pachyrhizi* was superior to the result achieved with the positive control (ZDMC) at 120 $\mu\text{mol L}^{-1}$.

Thus, the studies here described indicated that the allyldithiocarbamate salts are a new group of biologically active substances with potential application for the control of coffee leaf rust and Asian soybean rust diseases. Differently from dithiocarbamates such as ZDMC, the allyldithiocarbimates are metal free and form anionic species. We have shown that changes in the structure of the allylic anions can enhance the antifungal activity of their salts. The good results presented by these salts may be further improved by variations on the cation, what can modulate the salt solubility and the activity of this new class of agrochemicals. Compound **2c** is a target substance for further studies on the development of a new fungicide, especially considering the inhibition of *P. pachyrhizi* germination.

Supplementary Information

Supplementary crystallographic data for **2a** (CCDC 1559144) can be obtained free of charge from the Cambridge Crystallographic Data Centre via www.ccdc.cam.ac.uk/data_request/cif (or from the Cambridge Crystallographic Data Centre, 12, Union Road, Cambridge CB2 1EZ, UK; fax: +44 1223 336033).

Supplementary data are available free of charge at <http://jbcs.sbq.org.br> as PDF file.

Acknowledgments

We are grateful to the Fundação de Amparo à Pesquisa do Estado de Minas Gerais (FAPEMIG, grant APQ-02382-17), Conselho Nacional de Desenvolvimento Científico e Tecnológico (CNPq) and Coordenação de Aperfeiçoamento de Pessoal de Nível Superior (CAPES) for financial support and research fellowships. We thank the Núcleo de Análise de Biomoléculas of the Universidade Federal de Viçosa for providing the facilities for HRMS experiments.

References

- Hogarth, G.; *Prog. Inorg. Chem.* **2005**, *53*, 71.
- Kanemoto-Kataoka, Y.; Oyama, T. M.; Ishibashi, H.; Oyama, Y.; *Chem.-Biol. Interact.* **2015**, *237*, 80.
- Guo, X.; Zhou, S.; Chen, Y.; Chen, X.; Liu, J.; Ge, F.; Lian, Q.; Chen, X.; Ge, R. S.; *Toxicol. Sci.* **2017**, *160*, 329.
- Alves, L. C.; Rubinger, M. M. M.; Lindemann, R. H.; Perpétuo, G. J.; Janczak, J.; Miranda, L. D. L.; Zambolim, L.; Oliveira, M. R. L.; *J. Inorg. Biochem.* **2009**, *103*, 1045.
- Oliveira, A. A.; Oliveira, M. R. L.; Rubinger, M. M. M.; Rezende, D. C.; Zambolim, L.; *Quim. Nova* **2015**, *38*, 757.
- Vidigal, A. E. C.; Rubinger, M. M. M.; Oliveira, M. R. L.; Guilardi, S.; Souza, R. A. C.; Ellena, J.; Zambolim, L.; *J. Mol. Struct.* **2016**, *1114*, 21.
- Bomfim-Filho, L. F. O.; Oliveira, M. R. L.; Miranda, L. D. L.; Vidigal, A. E. C.; Guilardi, S.; Souza, R. A. C.; Ellena, J.; Ardisson, J. D.; Zambolim, L.; Rubinger, M. M. M.; *J. Mol. Struct.* **2017**, *1129*, 60.
- Tavares, E. C.; Rubinger, M. M. M.; Filho, E. V.; Oliveira, M. R. L.; Veloso, D. P.; Ellena, J.; Guilardi, S.; Souza, R. A. C.; Zambolim, L.; *J. Mol. Struct.* **2016**, *1106*, 130.
- Avelino, J.; Cristancho, M.; Georgiou, S.; Imbach, P.; Aguilar, L.; Bornemann, G.; Läderach, P.; Anzueto, F.; Hruska, A. J.; Morales, C.; *Food Secur.* **2015**, *7*, 303.
- Zambolim, L.; *Trop. Plant Pathol.* **2016**, *41*, 1.
- Godoy, C. V.; Seixas, C. D. S.; Soares, R. M.; Marcelino-Guimarães, F. C.; Meyer, M. C.; Costamilan, L. M.; *Pesq. Agropec. Bras.* **2016**, *51*, 407.
- Oliveira, M. R. L.; de Bellis, V. M.; *Transition Met. Chem.* **1999**, *24*, 127.
- Franca, E. F.; Oliveira, M. R. L.; Guilardi, S.; Andrade, R. P.; Lindemann, R. H.; Amim, J.; Ellena, J.; de Bellis, V. M.; Rubinger, M. M. M.; *Polyhedron* **2006**, *25*, 2119.
- Cunha, L. M. G.; Rubinger, M. M. M.; Sabino, J. R.; Visconte, L. L. Y.; Oliveira, M. R. L.; *Polyhedron* **2010**, *29*, 2278.
- Cai, J. X.; Zhou, Z. H.; Zhao, G. F.; Tang, C. C.; *Org. Lett.* **2002**, *4*, 4723.
- Ferreira, M.; Fernandes, L.; Sá, M. M.; *J. Braz. Chem. Soc.* **2009**, *20*, 564.
- Santhoshi, A.; Mahendar, B.; Mattapally, S.; Sadhu, P. S.; Banerjee, S. K.; Rao, V. J.; *Bioorg. Med. Chem. Lett.* **2014**, *24*, 1952.
- Bruker; *APEX2*; Bruker AXS Inc., Madison, WI, USA, 2004.
- Bruker; *SAINT*; Bruker AXS Inc., Madison, WI, USA, 2007.
- Bruker; *SADABS*; Bruker AXS Inc., Madison, WI, USA, 2002.
- Sheldrick, G. M.; *Acta Crystallogr., Sect. A* **2008**, *64*, 112.
- Sheldrick, G. M.; *Acta Crystallogr., Sect. C* **2015**, *71*, 3.
- Farrugia, L.; *J. Appl. Crystallogr.* **2012**, *45*, 849.
- Macrae, F.; Edgington, P. R.; McCabe, P.; Pidcock, E.; Shields, G. P.; Taylor, R.; Towler, M.; Van de Streek, J.; *J. Appl. Crystallogr.* **2006**, *39*, 453.
- Sebaugh, J. L.; *Pharm. Stat.* **2011**, *10*, 128.
- Vidigal, A. E. C.; Rubinger, M. M. M.; Queiroz, L. F.; Silva, L. F.; Zambolim, L.; Guilardi, S.; Souza, R. A. C.; Ellena, J.; Wetler, E. B.; Oliveira, M. R. L.; *Inorg. Chim. Acta* **2019**, *486*, 724.
- Allen, F. H.; Kennard, O.; Watson, D. G.; Brammer, L.; Orpen, A. G.; Taylor, R.; *J. Chem. Soc., Perkin Trans. 2* **1987**, *2*, S1.

28. Alves, L. C.; Rubinger, M. M. M.; Tavares, E. C.; Janczak, J.; Pacheco, E. B. A. V.; Visconte, L. L. Y.; Oliveira, M. R. L.; *J. Mol. Struct.* **2013**, *1048*, 244.
29. Durand, E.; Jacob, R. F.; Sherratt, S.; Lecomte, J.; Baréa, B.; Villeneuve, P.; Mason, R. P.; *Eur. J. Lipid Sci. Technol.* **2017**, *118*, 1600397.
30. Theodoridis, G.; *Adv. Fluorine Sci.* **2006**, *2*, 121.
31. Goulart, M. O. F.; Souza, A. A. S.; Abreu, F. C.; Paula, F. S.; Sales, E. M.; Almeida, W. P.; Buriez, O.; Amatore, C.; *J. Electrochem. Soc.* **2007**, *154*, 121.
32. de Paiva, Y. G.; de Souza, A. A.; Lima-Junior, C. G.; Silva, F. P. L.; Filho, E. B. A.; de Vasconcelos, C. C.; de Abreu, F. C.; Goulart, M. O. F.; Vasconcellos, M. L. A. A.; *J. Braz. Chem. Soc.* **2012**, *23*, 894.
33. Jeschke, P.; *Pest Manage. Sci.* **2017**, *73*, 1053.

Submitted: July 10, 2019

Published online: October 3, 2019

